# Simulation of wave motion and wave breaking induced energy dissipation

FRANCESCO GALLERANO, GIOVANNI CANNATA, LUCA BARSI, FEDERICA PALLESCHI, BENEDETTA IELE
Department of Civil, Constructional and Environmental Engineering
"Sapienza" University of Rome
Via Eudossiana 18, 00184
ITALY
francesco.gallerano@uniroma1.it https://www.dicea.uniroma1.it/users/francescogalleranouniroma1it

*Abstract:* - We propose a one-equation turbulence model based on a modified closure relation for the length scale of turbulence. The proposed model is able to adequately represent the energy dissipation due to the wave breaking and does not need any criterion to a priori locate the wave breaking point and the region in which the turbulence model has to be activated. The numerical simulation of wave transformation is carried out by solving the Navier-Stokes equations expressed in an integral formulation on a time dependent curvilinear coordinate system where the vertical coordinate varies in time and vectors and tensors are represented in a Cartesian base system. The model performance is assessed by numerically reproducing a laboratory test which consists in producing the breaking of a spilling wave on a sloping beach.

*Key-Words:* - three-dimensional model, time-dependent coordinate, wave propagation, wave breaking, turbulence model, energy dissipation.

## 1 Introduction

In recent years many models have been developed for the simulation of hydrodynamic phenomena related to wave motion. One of the most used methodology is based on the depth-averaged motion equations. Some of the most recent models based on this approach make use of the extended Boussinesq equations [1-3] to simulate the propagation of wave motion in deep and intermediate waters, where the dispersive effects are dominant, and make use of the nonlinear shallow water equations to simulate the wave breaking in the surf zone [4,5]. In the above models the necessity arises to introduce a criterion to establish where and when to switch from a system of equations to the other one.

A different methodology is based on three-dimensional models based on the numerical integration of the Navier-Stokes equations [6-10].

In the first three dimensional models for free surface flows, the Navier-Stokes equations were numerically integrated by using Cartesian coordinates and by adopting the volume of fluid technique (VOF) to track the location of discontinuous free surface [11-12].
By this way vertical fluxes cross the calculus cell arbitrarily: therefore, it is difficult to correctly assign the pressure boundary condition and the kinematic at free surface [13].

A more recent class of models [14] overcomes the above-mentioned drawbacks by mapping the physical Cartesian grid, that varies over time with the free surface movement, in a computational grid which has always a rectangular prismatic shape ($\sigma$-coordinate transformation [15]). By doing so, the free surface is always located at the upper computational boundary and its position can be determined by applying the free surface kinematic boundary condition. Furthermore, it is possible to assign the zero-pressure boundary condition at the free surface without any approximation [16-17].

These two aforementioned types of model are not able to directly simulate the breaking waves and consequently introduce, within the motion equations, turbulence models aimed to reducing the wave height in the surf zone. In order to avoid the numerical instabilities produced by the strong free surface elevation gradients, these models need to use highly dissipative turbulence models and to locate the initial break point by means of an "a priori" criterion. The main limitation of these models is given by the fact that they are not able to simulate the steep fronts related to the wave breaking and underestimate the wave height

Another type of model directly simulates the wave breaking, by introducing, in the $\sigma$-coordinates contest, shock-capturing methods that give the possibility of tracking the actual location of the start of wave breaking without requiring any criterion "a priori" [13, 16-18].

In the $\sigma$-coordinates shock capturing models the 3D motion equations are formulated in terms of cartesian based conserved variables on a time dependent coordinate system, in which the vertical coordinate varies in time ($\sigma$-coordinates 3D model). These models provide an excellent agreement between the numerical results and the experimental measures regarding the wave heights before breaking and the identification of the breaking itself, without the need of imposing "a priori" criterions aimed at localizing the initial break point.

As described by Derakhti et al. [19], the 3D shock-capturing models without any turbulence model, generally underestimate the specific energy dissipation at breaking and, consequently, overestimate the wave height in the surf zone.

In this paper, the numerical simulation of wave transformation relies on the resolution of the Navier-Stokes equations expressed in an integral formulation on a time dependent curvilinear coordinate system where the vertical coordinate varies in time and vectors and tensors are represented in a Cartesian base system. The pressure boundary conditions are placed on the upper face of each computational cell. The proposed integral formulation represents a generalization of the conservative differential formulation of the Navier-Stokes equations expressed in a $\sigma$-coordinate system.

In this paper we propose a modified $k-l$ turbulence model (where $k$ is the turbulent kinetic energy and $l$ is length scale of turbulence) which is able to adequately represent the energy dissipation due to the wave breaking.

Unlike the model of Bradford [12], in the proposed closure relation for the turbulent kinetic energy production, all the non-linear terms are taken into account. Furthermore, the proposed closure relation for the dissipation rate of the turbulent kinetic energy is expressed by a length scale of turbulence $l$, which is a function of the wave height. This choice allows as to formulate a $k-l$ turbulence model in which the length scale of the turbulence, $l$, does not depend on any empirical coefficient. Consequently, the proposed model does not need any criterion to "a priori" locate the wave breaking point and the region in which the turbulence model has to be activated.

# 2 The proposed model

## 2.1 Governing integral three-dimensional $\sigma$-coordinate equations

Let $(\xi^1,\xi^2,\xi^3,\tau)$ be a system of curvilinear coordinates, the transformation from Cartesian coordinates $(x^1,x^2,x^3)$ to the generalized curvilinear coordinates $(\xi^1,\xi^2,\xi^3)$ is:

$$\xi^1=\xi^1(x^1,x^2,x^3,t);\quad \xi^2=\xi^2(x^1,x^2,x^3,t)$$
$$\xi^3=\xi^3(x^1,x^2,x^3,t) \tag{1}$$

$\vec{g}_{(l)}=\partial\vec{x}/\partial\xi^l$ and $\vec{g}^{(l)}=\partial\xi^l/\partial\vec{x}$ are the covariant and contravariant base vectors.

The Jacobian of the transformation is given by $\sqrt{g}=\vec{g}_{(\alpha)}\cdot(\vec{g}_{(\beta)}\wedge\vec{g}_{(\gamma)})$.

$\Delta V(t)$ is considered as a volume element defined by surface elements bounded by curves lying on the coordinate. The volume element $\Delta V(t)=\Delta x^1\Delta x^2\Delta x^3=\sqrt{g}\Delta\xi^1\Delta\xi^2\Delta\xi^3$ is defined in the physical space that is time dependent and it is also defined the volume element in the transformed space $\Delta V^*=\Delta\xi^1\Delta\xi^2\Delta\xi^3$ that is not time dependent. In the same way it is indicated the surface element in the physical space $\Delta A(t)=\Delta x^\alpha\Delta x^\beta=\sqrt{g}\Delta\xi^\alpha\Delta\xi^\beta$ and the surface element in the transformed space $\Delta A^*=\Delta\xi^\alpha\Delta\xi^\beta$ ($\alpha,\beta=1,3$ are cyclic).

The Cartesian components of vector $\vec{n}dA^\alpha$, where $dA^\alpha$ is the surface element in which $\xi^\alpha$ is constant and $\vec{n}$ is the unit vector normal to $dA^\alpha$, can be written in the form

$$n_m dA^\alpha=g_m^{(\alpha)}\sqrt{g}\,d\xi^\beta d\xi^\gamma \tag{2}$$

in which $\alpha,\beta,\gamma$ are cyclic. Let $h$ be the still water level, $H$ the total water depth and $\eta(x^1,x^2,t)=H(x^1,x^2,t)-h(x^1,x^2,t)$ the free surface elevation with respect to the still water level $h$.

We define $u_m$ as the Cartesian components of the fluid velocity, $v_m$ the Cartesian components of the velocity of the control volume, $G$ the constant of gravity, $q$ the dynamic pressure and $T_{lm}$ the Cartesian components of the stress tensor.

In order to simulate the fully dispersive wave processes and accurately assigned the dynamic and kinematic boundary conditions at the free surface, we adopt the following transformation from Cartesian coordinates to curvilinear ones, in which the vertical coordinate varies in time so as the follow the time variation of the free surface elevation

$$\xi^1=x^1;\quad \xi^2=x^2;\quad \xi^3=\frac{x^3+h}{H};\quad \tau=t \tag{3}$$

The following relation is valid:

$$v_3 = \frac{\partial x^3}{\partial \tau} \tag{4}$$

This coordinate transformation basically maps the varying vertical coordinates in the physical domain to a uniform transformed space where $\xi^3$ spans from 0 to 1. In addition, the Jacobian of the transformation becomes

$$\sqrt{g} = H \tag{5}$$

We define the cell-averaged value (in the transformed space) of primitive variable and conservative one

$$\begin{aligned} \overline{H} &= \frac{1}{\Delta V^*}\int_{\Delta V} H d\xi^1 d\xi^2 d\xi^3 \\ \overline{Hu_l} &= \frac{1}{\Delta V^*}\int_{\Delta V^*} H u_l d\xi^1 d\xi^2 \, d\xi^3 \end{aligned} \tag{6}$$

By using Eqs. (5) and (6) the momentum equation can be expressed in the form [17]

$$\begin{aligned} &\frac{\partial \overline{Hu_l}}{\partial \tau} = -\frac{1}{\Delta V^*}\sum_{\alpha=1}^{3} \\ &\left\{\int_{\Delta A^{*\alpha+}}\left[u_l(u_m - v_m) g_m^{(\alpha)} H\right] d\xi^\beta d\xi^\gamma \right. \\ &\left. - \int_{\Delta A^{*\alpha-}}\left[u_l(u_m - v_m) g_m^{(\alpha)} H\right] d\xi^\beta d\xi^\gamma \right\} \\ &-\frac{1}{\Delta V^*}\sum_{\alpha=1}^{3}\left\{\int_{\Delta A^{*\alpha+}}\left[G\eta g_m^{(\alpha)} H\right] d\xi^\beta d\xi^\gamma \right. \\ &\left. - \int_{\Delta A^{*\alpha-}}\left[G\eta g_m^{(\alpha)} H\right] d\xi^\beta d\xi^\gamma \right\} \\ &-\frac{1}{\Delta V^*}\frac{1}{\rho}\int_{\Delta V^*}\frac{\partial q}{\partial \xi^\alpha} g_m^{(\alpha)} H d\xi^1 d\xi^2 d\xi^3 \\ &-\frac{1}{\Delta V^*}\sum_{\alpha=1}^{3}\left\{\int_{\Delta A^{*\alpha+}}\left[\frac{T_{lm}}{\rho} g_m^{(\alpha)} H\right] d\xi^\beta d\xi^\gamma \right. \\ &\left. - \int_{\Delta A^{*\alpha-}}\left[\frac{T_{lm}}{\rho} g_m^{(\alpha)} H\right] d\xi^\beta d\xi^\gamma \right\} \end{aligned} \tag{7}$$

Where $\Delta A^{*\alpha+}$ and $\Delta A^{*\alpha-}$ indicate the contour surfaces of the volume element $\Delta V^*$ on which $\xi^\alpha$ is constant and which are located at the larger and the smaller value of $\xi^\alpha$ respectively.

Here the index $\alpha, \beta$ and $\gamma$ are cyclic. The total time derivative on the left side hand of (7)) became a local time derivative because the integral is a function of $(\xi^1, \xi^2, \xi^3, \tau)$. It is possible to see that the time varying of geometric components is expressed by the metric terms.

By integrating the continuity equation over the water column and applying the bottom and surface kinematic boundary conditions, we obtain

$$\begin{aligned} &\frac{\partial \overline{H}}{\partial \tau} + \frac{1}{\Delta A^*_{xy}}\int_0^1 \sum_{\alpha=1}^{3}\left[\int_{\Delta \xi^{\alpha+}} H u_\alpha d\xi^\beta \right. \\ &\left. - \int_{\Delta \xi^{\alpha-}} H u_\alpha d\xi^\beta \right] d\xi^3 = 0 \end{aligned} \tag{8}$$

in which $\xi^{\alpha+}$ and $\xi^{\alpha-}$ indicate the contour line of the surface element $\Delta A^*$ on which $\xi^\alpha$ is constant and which are located at the larger and the smaller value of $\xi^\alpha$ respectively. $\Delta A^*_{xy} = \Delta\xi^1 \Delta\xi^2$ is the horizontal surface element in the transformed space. This equation represents the governing equation for the surface movements. Equations (7)) and (8)) represent the three-dimensional motion equations in time dependent coordinate system $(\xi^1, \xi^2, \xi^3, \tau)$ in which the variables are $\overline{Hu_l}$ and $\overline{H}$ .

Equations (7) and (8) are numerically solved by means of a finite-volume shock-capturing scheme which uses an approximate HLL Riemann solver. The solution of the system formed by Equations (7) and (8) is advanced in time by using a three-stage strong-stability-preserving Runge-Kutta (SSPRK) fractional step method. Further details on the numerical scheme can be found in [16].

### 2.2 Turbulence model

By adopting the same time dependent curvilinear coordinate system, the integral form of the turbulent kinetic energy transport equation reads

$$\begin{aligned} &\frac{\partial \overline{Hk}}{\partial \tau} = \\ &-\frac{1}{\Delta V^*}\sum_{\alpha=1}^{3}\left\{\int_{\Delta A^{*\alpha+}}\left[k(u_m - v_m) g_m^{(\alpha)} H\right] d\xi^\beta d\xi^\gamma \right. \\ &\left. - \int_{\Delta A^{*\alpha-}}\left[k(u_m - v_m) g_m^{(\alpha)} H\right] d\xi^\beta d\xi^\gamma \right\} \\ &-\frac{1}{\Delta V^*}\sum_{\alpha=1}^{3}\left\{\int_{\Delta A^{*\alpha+}}\left[\left(\nu + \frac{\nu_T}{\sigma_k}\right)\frac{\partial k}{\partial \xi^\alpha} g_m^{(\alpha)} g_n^{(\alpha)} H\right] d\xi^\beta d\xi^\gamma \right. \\ &\left. - \int_{\Delta A^{*\alpha-}}\left[\left(\nu + \frac{\nu_T}{\sigma_k}\right)\frac{\partial k}{\partial \xi^\alpha} g_m^{(\alpha)} g_n^{(\alpha)} H\right] d\xi^\beta d\xi^\gamma \right\} \end{aligned} \tag{9}$$

$$-\frac{1}{\Delta V^*}\int_{\Delta V^*}(P-\varepsilon)Hd\xi^1d\xi^2d\xi^3$$

where $k$ is the turbulent kinetic energy, $\varepsilon$ is the dissipation rate, $P$ is the turbulent kinetic energy production, $\nu$ is the viscosity of the fluid, $\nu_T$is the turbulent eddy viscosity and $\sigma_k$ is a coefficient.

The dissipation rate is expressed in the form of

$$\varepsilon=\frac{k^{3/2}}{l} \tag{10}$$

and the turbulent eddy viscosity is given by

$$\nu_T=C_\mu\sqrt{k}l \tag{11}$$

where $C_\mu$ is an empirical coefficient and $l$ is the length scale of turbulence.

In the work of Bradford [12] the length scale $l$ is expressed as $l=\phi h$, in which $\phi=0.1$ and $h$ is the still water depth. This choice implies that the length scale of turbulence $l$ is high before breaking and excessively decreases downstream the initial break point. Consequently (as shown in Section 3) this model proves to be excessively dissipative before the breaking (where it underestimates the wave height), while it vanishes in the shallow water zones downstream the break point (where the wave heights result to be overestimated).

In this work, in order to overcome the drawback of the model proposed by Bradford, we propose an original closure relation for the length scale of turbulence $l$. Let $\xi^2$ the curvilinear coordinate approximately parallel to the shoreline and $\xi^1$ the curvilinear coordinate approximately orthogonal to it. Let $T$ be the wave period. We define $\eta_{max}(\xi^1,\xi^2)=\max_t\eta(\xi^1,\xi^2,t)$ and $\eta_{min}(\xi^1,\xi^2)=\min_t\eta(\xi^1,\xi^2,t)$, where $t\in T$.

Let be the local wave height as $\lambda(\xi^1,\xi^2)=\eta_{max}(\xi^1,\xi^2)-\eta_{min}(\xi^1,\xi^2)$ the local maximum water depth as $H^*(\xi^1,\xi^2)=\eta_{max}(\xi^1,\xi^2)+h(\xi^1,\xi^2)$ and the maximum wave height as $\lambda^*(\xi^2)=\max_{\xi^1}\lambda(\xi^1,\xi^2)$.

The length scale of turbulence is given by

$$l(\xi^1,\xi^2)=\lambda^*(\xi^2)\frac{\lambda(\xi^1,\xi^2)}{H^*(\xi^1,\xi^2)} \tag{12}$$

Furthermore, in the proposed model, the turbulent kinetic energy production term is given by

$$P=\int_{\Delta V^*}-T_{lm}\frac{\partial u_m}{\partial\xi^\alpha}g_m^{(\alpha)}Hd\xi^1d\xi^2d\xi^3 \tag{13}$$

in which the Reynolds stress tensor $T_{lm}$ is expressed by a non-linear model proposed by Lin and Liu [20].

$$\begin{aligned}T_{lm}=&-C_d\frac{k^2}{\varepsilon}\left(\frac{\partial u_l}{\partial\xi^\alpha}g_m^{(\alpha)}+\frac{\partial u_m}{\partial\xi^\alpha}g_l^{(\alpha)}\right)+\frac{2}{3}k\delta_{lm}\\&-C_1\frac{k^3}{\varepsilon^2}\left\{\left[\left(\frac{\partial u_l}{\partial\xi^\alpha}g_m^{(\alpha)}\frac{\partial u_l}{\partial\xi^\alpha}g_m^{(\alpha)}\right)+\left(\frac{\partial u_m}{\partial\xi^\alpha}g_l^{(\alpha)}\frac{\partial u_m}{\partial\xi^\alpha}g_l^{(\alpha)}\right)\right]-\frac{2}{3}\left(\frac{\partial u_l}{\partial\xi^\alpha}g_m^{(\alpha)}\frac{\partial u_l}{\partial\xi^\alpha}g_m^{(\alpha)}\right)\delta_{lm}\right\}\\&-C_2\frac{k^3}{\varepsilon^2}\left\{\left(\frac{\partial u_l}{\partial\xi^\alpha}g_m^{(\alpha)}\frac{\partial u_m}{\partial\xi^\alpha}g_l^{(\alpha)}\right)-\frac{1}{3}\left(\frac{\partial u_l}{\partial\xi^\alpha}g_m^{(\alpha)}\frac{\partial u_m}{\partial\xi^\alpha}g_l^{(\alpha)}\right)\delta_{lm}\right\}\\&-C_3\frac{k^3}{\varepsilon^2}\left\{\left(\frac{\partial u_m}{\partial\xi^\alpha}g_l^{(\alpha)}\frac{\partial u_l}{\partial\xi^\alpha}g_m^{(\alpha)}\right)-\frac{1}{3}\left(\frac{\partial u_m}{\partial\xi^\alpha}g_l^{(\alpha)}+\frac{\partial u_l}{\partial\xi^\alpha}g_m^{(\alpha)}\right)\delta_{lm}\right\}\end{aligned} \tag{14}$$

where the coefficients $C_d$, $C_1$, $C_2$ and $C_3$ are

$$C_d=\frac{2}{3}\left(\frac{1}{7.4+2S_{max}}\right);C_1=\frac{1}{185.2+3D_{max}^3};\quad C_2=-\frac{1}{58.8+2D_{max}^2};C_3=\frac{1}{370.4+3D_{max}^2} \tag{15}$$

in which

$$S_{max}=\frac{k}{\varepsilon}max\left\{\left|\frac{\partial u_l}{\partial\xi^\alpha}g_l^{(\alpha)}\right|\right\}\text{ (indices not summed)}\qquad D_{max}=\frac{k}{\varepsilon}max\left\{\left|\frac{\partial u_l}{\partial\xi^\alpha}g_m^{(\alpha)}\right|\right\} \tag{16}$$

# 3 Results

In this section, the laboratory test performed by Thing and Kirby [21], is numerically reproduced. This test consists in realizing a spilling wave breaking on a sloping beach. By means of this test, the role of the turbulence model on the wave energy dissipation processes in the surf zone is examined. Fig. 1 shows a schematic representation of the experimental arrangement.

The numerical simulations are performed by means of a computational grid whose cell number is 13728. A grid spacing $\Delta x=0.025m$ is used in the horizontal direction, while 13 layers are used in the vertical direction. At the western boundary, a cnoidal wave train is generated whose height in the

constant-depth water region is $H = 0.125m$ and the period is $T = 2s$.

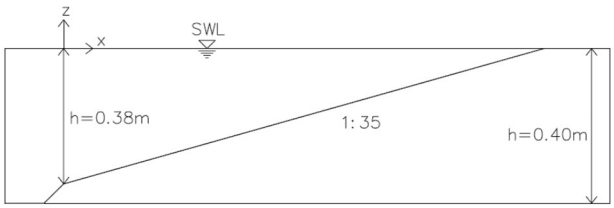


Fig. 1 - Experimental arrangement of Ting and Kirby [21]

Fig. 2 shows the distribution of the wave crest and wave trough along the cross-shore direction, together with the mean water level, obtained by the proposed numerical model in which the turbulent stress terms are switched off. Fig. 2 also shows the corresponding quantities obtained experimentally by Ting and Kirby [21] and numerically by Ma et al. [13]. By observing Fig. 2 it is possible to notice that the numerical results fit quite well the experimental data in the shoaling zone: as far the model presented in Ma et al. [13], only a slight overestimation of the wave crest results from the simulation. By observing Fig. 2 it is also possible to see that the proposed model provides an early initiation of the wave breaking in the case in which the turbulent stress terms are switched off. With respect to the model presented by Ma et al. [13], this early initiation of wave breaking is slightly less pronounced. Lastly, Fig. 2 shows that, if turbulence stress terms are switched off, the proposed model overestimates the wave crest in the surf zone: this overestimation is very close to that obtained by the model of Ma et al. [13].

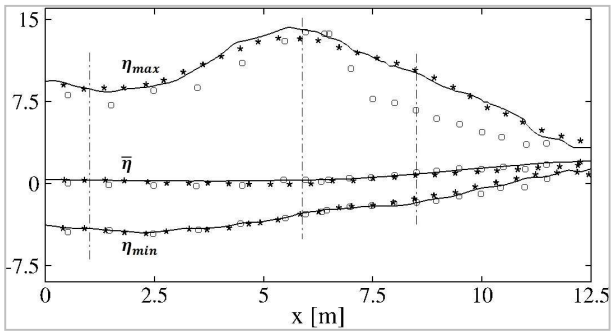


Fig. 2 – Mean water level and distribution of crest and trough elevations along the cross-shore direction for the surf zone spilling breaking case of Ting and Kirby [21]. Comparison between experimental data (empty circles), numerical results from Ma et al. [13] (cross) and numerical results obtained by the proposed model without turbulence model (solid line).

Fig. 3 shows the cross-shore distribution of the wave crest and the wave trough and the mean water level obtained by including the turbulent stress terms in the proposed model. Fig. 3 also shows the corresponding quantities obtained experimentally by Ting and Kirby [21] and numerically by Bradford [12]. For this test, Bradford [12] used a VOF technique for the free surface elevation and a one-equation turbulence model in which the length scale of turbulence is given by $l = 0.1h$. In the model proposed by Bradford, the dissipation rate $\varepsilon$ increases as $l$ reduces, and both the turbulent kinetic energy and the turbulent kinematic viscosity decrease. This provides an overestimation of the crest and trough elevation in the shallow water zone, as shown in Fig. 3. Furthermore, in the zone before breaking, the model proposed by Bradford provides underestimated values of the crest and trough elevation with respect to the experimentally measured data. In order to overcome these limitations, in the proposed turbulence model the direct dependence of $l$ from the still water depth is suppressed and the length scale of turbulence is expressed as a function of the wave height. By observing Fig. 3 it is possible to notice that the modified $k - l$ turbulence model proposed in this work well fits the experimental distribution of the wave crest both before and after the breaking. Furthermore, by comparing Fig. 2 and Fig. 3 it is evident how, with respect to the results obtained without including the turbulence stress terms, the turbulence model proposed in this work provides a better estimation of the break point location and correctly predicts the wave height in the entire surf zone.

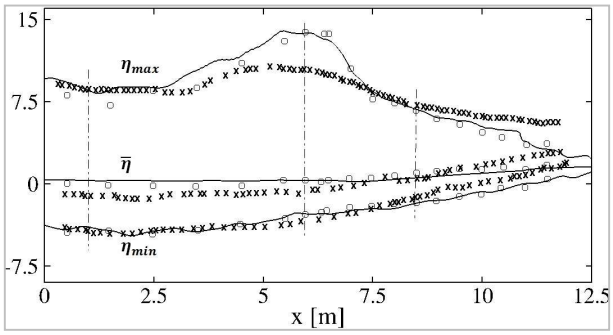


Fig. 3 - Mean water level and distribution of crest and trough elevations along the cross-shore direction for the surf zone spilling breaking case of Ting and Kirby [21]. Comparison between experimental data (empty circles), numerical results from Bradford [12] (cross) and numerical results obtained by the proposed model with the modified $k - l$ (solid line)

Fig. 4a-c show the time evolution of the water surface elevation, during a time interval equal to the wave period, evaluated respectively at $x = 1m$ (after the toe of the slope), $x = 5.95m$ (before the break point) and $x = 8.49m$ (after the break point). For each of these figures, numerical results (obtained with and without including the turbulence stress terms) and experimental data are reported. By observing Fig. 4a and Fig. 4b, it is evident that the turbulence model proposed in this work has not significant effect on the solution before the break point. From Fig. 4c it can be deduced that in the surf zone the wave heights predicted without using any turbulence model are overestimated with respect to the experimental data. On the other hand, the wave heights predicted by using the proposed turbulence model are in good agreement with the experimental data.

Figs. 5a-c show an instantaneous wave field along the cross-shore direction. Fig. 5a shows the time-varying computational grid in which the lower and upper layers are refined in order to improve the accuracy of the numerical solution near the bottom and the free surface. Figs. 5b and 5c show an instantaneous representation of the velocity vectors and the turbulent kinetic energy contours respectively. From Figure 5b it is possible to see that the proposed model is able to capture the steeping of the wave fronts as the wave train approach the shore, and the increasing of the vertical velocity component which occurs as the wave front steepen. Fig. 5c shows how the turbulence model mainly acts in the surf zone, where the wave turbulence processes are significant, while it has no significant effect before the break point (shoaling zone).

# 4 Conclusion

In this work, a modified $k - l$ turbulence model (where $k$ is the turbulent kinetic energy and $l$ is length scale of the turbulent eddies) has been proposed which is able to adequately represent the energy dissipation due to the wave breaking. The model performance has been assessed by numerically reproducing a laboratory test which consists in realizing the breaking of a spilling wave on a sloping beach. It has been shown that the proposed turbulence model spontaneously activates after the break point, where the wave turbulence processes are significant, and makes it possible to avoid the significant underprediction of the energy dissipation induced by the wave breaking in the surf zone, which is observed when no turbulence stress terms are included in the numerical simulation.

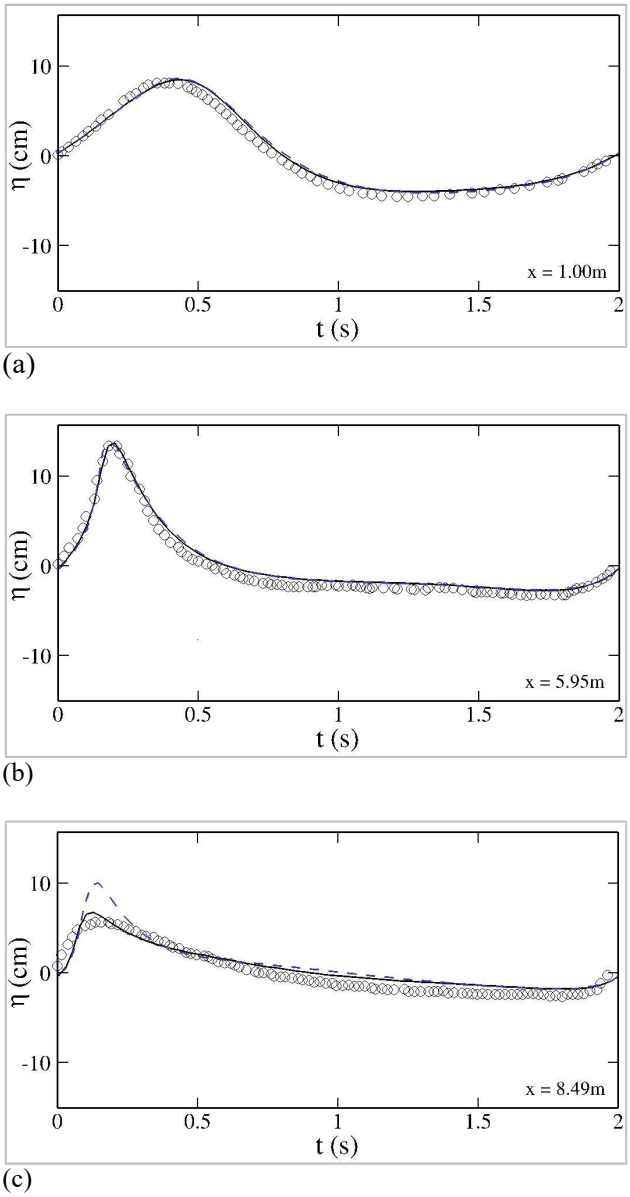


Fig. 4 – Phase-averaged water surface elevations for the surf-zone spilling breaking case at different cross shore locations. Comparison between experimental data (empty circles), numerical results obtained by the proposed model without turbulence model (dashed line) and numerical results obtained by the proposed model with the modified $k - l$ (solid line).

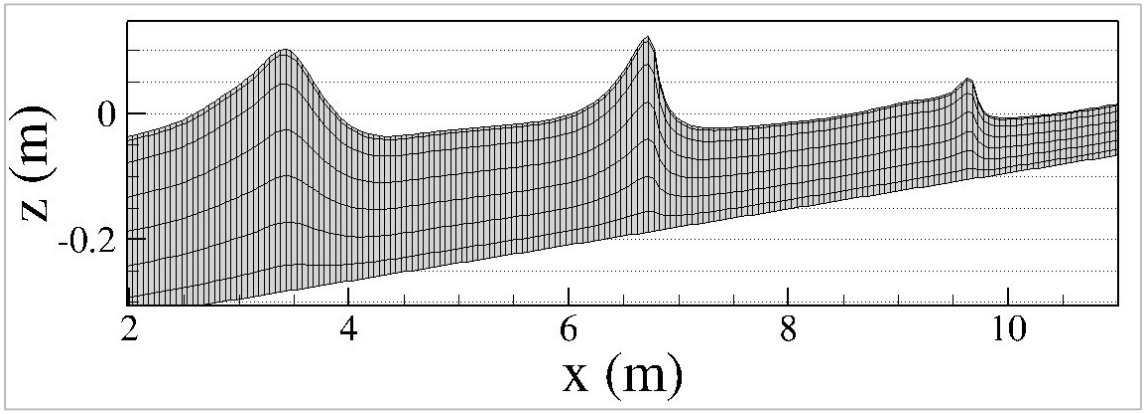


(a)

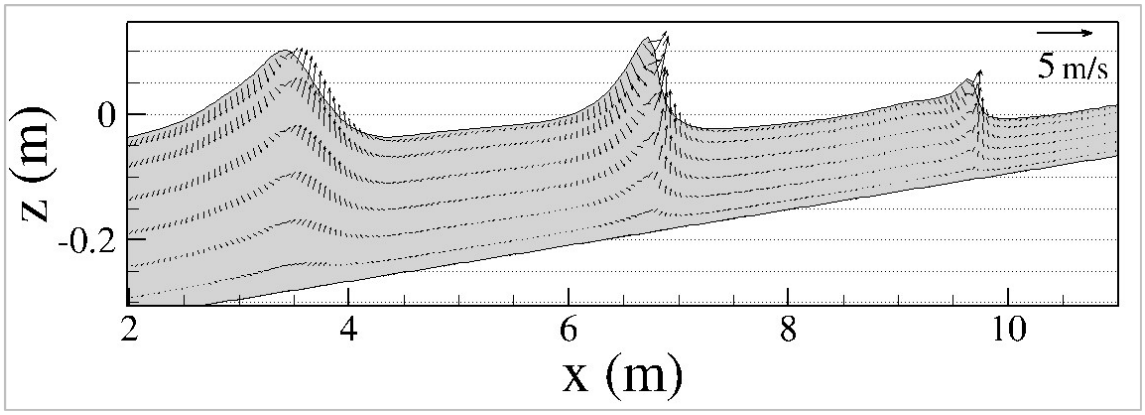


(b)

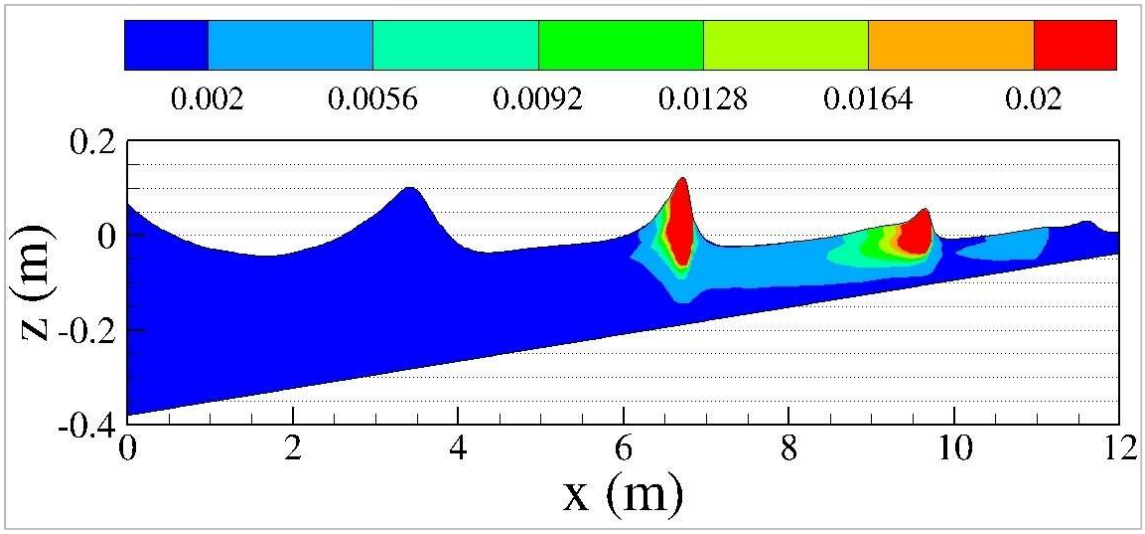


(c)

Fig. 5 - Instantaneous representations of: (a) computational grid, (b) velocity vectors, (c) turbulence kinetic energy obtained in the modified $k - l$ model.

*References:*

[1] G. Cannata, L. Barsi, C. Petrelli, and F. Gallerano, "Numerical investigation of wave fields and currents in a coastal engineering case study", *WSEAS Transactions on Fluid Mechanics*, Vol.13, 2018, pp. 87-94.

[2] F. Shi, J.T. Kirby, J.C. Harris, J.D. Geiman, and S. T. Grilli, "A high-order adaptive time-stepping TVD solver for Boussinesq modelling of breaking waves and coastal inundation", *Ocean Modelling*, Vol.43-44, 2012, pp. 36-51.

[3] F. Gallerano, G. Cannata, O. De Gaudenzi, and S. Scarpone, "Modeling Bed Evolution Using Weakly Coupled Phase-Resolving Wave Model and Wave Averaged Sediment Transport Model", *Coastal Engineering Journal*, Vol. 58, No.3, 2016, pp. 1650011-1-1650011-50, Article number 1650011.

[4] G. Cannata, F. Lasaponara, and F. Gallerano, "Non-linear Shallow Water Equations numerical investigation on curvilinear boundary-conforming grids", *WSEAS Transactions on Fluid Mechanics*, Vol.10, 2015, pp. 13-25.

[5] G. Cannata, C. Petrelli, L. Barsi, F. Fratello, and F. Gallerano, "A dam-break flood simulation model in curvilinear coordinates", *WSEAS Transactions on Fluid Mechanics*, Vol.13, 2018, pp. 60-70.

[6] X. Chen, "A fully hydrodynamic model for three-dimensional free-surface flows", *International Journal for Numerical Methods in Fluids*, Vol.42, 2003, pp. 929-952.

[7] G. Cannata, L. Barsi, and F. Gallerano, "Numerical investigation of the coupled flutter onset mechanism for streamlined bridge deck cross-sections", *WSEAS Transactions on Fluid Mechanics*, Vol.12, 2017, pp. 43-52.

[8] G. Cannata, L. Barsi, and F. Gallerano, "Numerical simulation of the coupled flutter instability for closed-box bridge decks", *International Journal of Mechanics*, Vol.11, 2017, pp. 128-140.

[9] A. Cantelli, P. Monti, and G. Leuzzi, "Numerical study of the urban geometrical representation impact in a surface energy budget model", *Environmental Fluid Mechanics*, Vol.15, 2015, pp. 251-273.

[10] A. Amicarelli, G. Leuzzi, and P. Monti, "A comparison between IECM and IEM Lagrangian models", *International Journal of Environment and Pollution*, Vol.44, Nos.1-2-3-4, 2011, pp. 324-331.

[11] F.H. Harlow, and J.E. Welch, "Numerical Calculation of Time-Dependent Viscous Incompressible Flow of Fluid with Free Surface", *Physics of Fluids*, Vol.8, No.12, 1965, pp. 2182-2189.

[12] S.F. Bradford, "Numerical Simulation of Surf Zone Dynamics", *Journal of Waterway Port Coastal and Ocean Engineering*, Vol.126, No.1, 2000, pp. 1-13.

[13] G.Ma, F. Shi, and J.T. Kirby, "Shock-capturing non-hydrostatic model for fully dispersive surface wave processes", *Ocean Modelling*, Vol.43-44, 2012, pp. 22-35.

[14] H. Yuan, and C.H. Wu, "A two-dimensional vertical non-hydrostatic σ model with implicit method for free-surface flows", *International Journal for Numerical Methods in Fluids*, Vol.44, 2004, pp. 811-835.

[15] N.A. Phillips, "A coordinate system having some special advantages for numerical forecasting", *Journal of Meteorology*, Vol.14, 1956, pp. 184-185.

[16] G. Cannata, C. Petrelli, L. Barsi, F. Camilli, and F. Gallerano, "3D free surface flow simulations based on the integral form of the equations of motion", *WSEAS Transactions on Fluid Mechanics*, Vol.12, 2017, pp. 166-175.

[17] G. Cannata, F. Gallerano, F. Palleschi, C. Petrelli, and L. Barsi, "Three-dimensional numerical simulation of the velocity fields induced by submerged breakwaters", *International Journal of Mechanics*, Vol.13, 2019, pp. 1-14.

[18] F. Gallerano, G. Cannata, F. Lasaponara, and C. Petrelli, "A new three-dimensional finite-volume non-hydrostatic shock-capturingt model for free surface flow", *Journal of Hydrodynamics*, Vol. 29, No.4, 2017, pp. 552-566.

[19] M. Derakhti, J.T. Kirby, F. Shi, and G. Ma, "NHWAVE:Consistent boundary conditions and turbulence modelling", *Ocean Modelling*, Vol.106, 2016, pp. 121-130.

[20] P. Lin, and P.L.-F. Liu, "A numerical study of breaking waves in the surf zone", *Journal of Fluid Mechanics*, Vol.359, 1998, pp.239-264.

[21] F. C. K. Ting and J.T. Kirby, "Observation of undertow and turbulence in a wave period", *Costal Engineering*, No.24, 1994, pp. 51-80.